Journal of Physics B: Atomic, Molecular and Optical Physics

PAPER

Rotational excitation of N_2 by positron impact in the adiabatic rotational approximation

To cite this article: Marcos V Barp *et al* 2018 *J. Phys. B: At. Mol. Opt. Phys.* **51** 205201

IOP Publishing Journal of Physics B: Atomic, Molecular and Optical Physics
J. Phys. B: At. Mol. Opt. Phys. **51** (2018) 205201 (9pp) https://doi.org/10.1088/1361-6455/aade81

Rotational excitation of N_2 by positron impact in the adiabatic rotational approximation

Marcos V Barp[1], Eliton Popovicz Seidel[1], Felipe Arretche[1] and Wagner Tenfen[2]

[1] Departamento de Física, Universidade Federal de Santa Catarina, 88040-900, Florianópolis, Santa Catarina, Brazil
[2] Departamento de Física, Universidade Federal da Fronteira Sul, 85770-000, Realeza, Paraná, Brazil

E-mail: marcos.barp@posgrad.ufsc

Received 4 May 2018, revised 30 August 2018
Accepted for publication 3 September 2018
Published 24 September 2018

Abstract

In this article we present the rotational excitation cross sections of N_2 by positron impact for energies between 1 and 10 eV. The cross sections were computed in the adiabatic rotational approximation within the many-body formalism of the Schwinger multichannel method. Our results show fortuitous agreement with previous rovibrational closed-coupling calculation and are higher in magnitude when compared to other similar calculation performed within the rigid rotor approximation. The convergence of static and static plus polarisation treatments suggests that dependence of polarisation for hexadecapole transitions may be neglected.

Keywords: positron scattering, rotational excitation, adiabatic approximation

(Some figures may appear in colour only in the online journal)

1. Introduction

Since the development of positron sources for experimental manipulation [1–3], the positron interaction with atoms and molecules has been a fascinating theme of investigation [4–9]. Among many atomic and molecular species, there is specific interest in the comprehension of the positron cooling dynamics in molecular nitrogen.

From the experimental point of view, N_2 is a non-toxic gas of easy acquisition and manipulation. In the theoretical context, on the other side, N_2 works, together with H_2, as a model system to test theories and approximations because of its moderate number of electrons and a relatively simple vibrational and rotational structure.

In 1970, Tao [10] presented experimental results for the positron annihilation spectra as a function of nitrogen densities. After, Coleman *et al* [11] and Griffith and Heyland [12] measured the positron lifetime spectra for molecular nitrogen at room temperature. In the same period, Sharma and McNutt [13] presented results for the annihilation spectra at 77 K. All these works verified that a significant amount of positrons, originally created in the radioactive decay with energies of order of keV's [2, 14], survive to energies below the positronium formation threshold (≈10 eV). It became evident that a satisfactory understanding of the experimental data, demanded first a comprehension of the dynamics of positron thermalisation in the gaseous system.

Below the positronium formation threshold, positrons interacting with this gas cool by momentum transfer, vibrational excitation and rotational excitation. The thermalisation dynamics of positrons in molecular nitrogen was studied by Coleman *et al* [15] using a simple slowing-down model. These authors worked with energies below the first vibrational threshold (≈0.290 eV). Effective rotational and momentum transfer cross sections were inferred comparing the cooling model with the measured annihilation time spectrum.

The development of high resolution low energy positron beams demanded the construction of an experimental apparatus able to cool and to trap these particles. Murphy and Surko [14] presented a modified Penning trap in what molecular nitrogen was used as buffer-gas. Along the years this

apparatus has been improved. For a good review on the state of the art on this subject see Natisin *et al* [16]. The performance of the positron trap has been modelled through empirical formulations along the time. To develop a consistent model of positron cooling in N_2, the knowledge of the vibrational and rotational cross sections is mandatory, mainly toward low energies [17].

The research reported in this article is about how positrons are able to make N_2 molecules rotate. More modernly, Natisin *et al* [18] measured the cooling curve of positrons with initial temperatures of the order of ≈1200 K in N_2 at room temperature. In this scenario, practically all the molecules are in the vibrational ground state, such that the experimental data work as an indirect measure of the rotational cross sections in the very low energy domain.

As far as we know, direct measurements of positron-N_2 rotational cross sections are not available until today. Nonetheless, the theme has attracted the attention of theorists [19–21] since the 70s and, from time to time, improved calculations were reported in literature. Of direct interest to us here are the cross sections reported by Mukherjee *et al* [22], del Valle and Gianturco [5] and Mukherjee and Mukherjee [23]. In spite of using similar correlation-polarisation potentials, the rotational cross sections reported by these authors are significantly different in the energy region we consider here. Motivated by this context, we understand that the positron-N_2 rotational cross sections are not well determined and that a theoretical investigation with a different methodology compared to the ones previously applied may contribute significantly to the problem.

This article is organised as follows: in section 2, we briefly present the methodology used to compute the rotational cross sections; in section 3, the results obtained are shown and discussed, and finally, in section 4, we state our conclusions. Unless otherwise stated, we use atomic units.

2. Theoretical methods

The rotational cross sections presented here have been calculated with the Schwinger multichannel method (SMC) [24] combined with the adiabatic rotational approximation (ARA) [25]. Details can be found in the article of Zanin *et al* [26], therefore only the essential points are given here.

The effective expression used to compute the rotational cross sections is

$$\sigma^{J_i\to J_f} = \frac{1}{4\pi}\frac{k_f}{k_i}\sum_{l_f\,l_i}\sum_{m\,n}(-1)^{m+n} f^{l_i m}_{l_f m}\,(f^{l_i\,n}_{l_f\,n})^* \times \sum_j C(J_i\,j\,J_f;\,0\,0\,0)^2 C(l_f\;l_i\,j;\,-m\;m\;0) \times C(l_f\;l_i\,j;\,-n\;n\;0), \quad (1)$$

where J_i and J_f are respectively the initial and final rotational states, the C's are the usual Clebsch–Gordan coefficients, k_f and k_i are the final and initial positron momenta and

$$f^{l_i m_i}_{l_f m_f}(\vec{k}_f,\vec{k}_i) = \int d\hat{k}_i \int d\hat{k}_f\, f^{BF} \times [\vec{k}_f,\vec{k}_i]\, Y^*_{l_f m_f}(\hat{k}_f)\, Y_{l_i m_i}(\hat{k}_i) \quad (2)$$

are the components of the body-frame scattering amplitude $f^{BF}[\vec{k}_f,\vec{k}_i]$ expanded in the angular momentum components of scattering wave vectors $\vec{k}_i$ and $\vec{k}_f$.

The body-frame scattering amplitude $f^{BF}[\vec{k}_f,\vec{k}_i]$ is originally computed in the linear momentum representation using the SMC [24]. In this method, the effective expression used to calculate the body-frame scattering amplitude is:

$$f[\vec{k}_f,\vec{k}_i] = -\frac{1}{2\pi}\sum_{mn}\langle S_{\vec{k}_f}|V|\chi_m\rangle (d^{-1})_{mn}\langle\chi_n|V|S_{\vec{k}_i}\rangle, \quad (3)$$

where

$$d_{mn} = \langle\chi_m|PVP + Q\hat{H}Q - VG^{(+)}_P V|\chi_n\rangle. \quad (4)$$

In these expressions, $S_{\vec{k}}$ is a solution of the unperturbed Hamiltonian (molecular Hamiltonian plus the kinetic energy operator for the incident positron), P and Q are projectors onto energetically open and closed states of the target, V is the scattering potential, $\hat{H}$ is the total energy minus the scattering Hamiltonian, $G^{(+)}_P$ is the projected Green's function and $\{\chi_{m\equiv\mu\nu}\}$ are the $(N+1)$-particle trial scattering functions which have the form

$$\chi_{m=\mu\nu} = \Phi_\mu(\vec{r}_j)\times\varphi_\nu(\vec{x}) \quad (5)$$

with $\Phi_\mu(\vec{r}_j)$ being the μth state of the target and $\varphi_\nu(\vec{x})$ the νth positron scattering orbital.

The ground state target wave function $\Phi_0(\vec{r}_j)$ is a restricted Hartree–Fock (RHF) one obtained from a self consistent field (SCF) calculation. As usual, the molecular orbitals are formed by linear combination of atomic orbitals, in this case, Cartesian Gaussian functions (CGF). The set of positron scattering orbitals $\{\varphi_\nu(\vec{x})\}$ is taken as the own set of occupied and virtual orbitals generated in the SCF calculation.

Due to the nature of the ARA, it is expected that it produces reliable results only above a certain energy. The central idea of the ARA is that, if the time spent by the projectile while crossing the target field is sufficiently small compared to the time associated to rotational transitions (or significant variations of the molecular orientation in space), then the electronic and the rotational molecular degrees of freedom can be decoupled in the scattering calculation. Comparing the time taken by the positron to cross a region of ≈20 a_0 (an overestimated value for the positron-N_2 potential range, see figure 4 of Tenfen *et al* [27]) to the classical period of rotation of the N_2 molecule or to the time uncertainty associated to quadrupole transitions ($J_f = J_i \pm 2$), we find that the results provided by the ARA are certainly valid for incident energies above 1 eV.

2.1. Computational details

The initial input used in a standard SMC calculation is a set of CGF. This set is used to generate the molecular ground state wave function and the excited determinants associated to the

Table 1. Cartesian Gaussian basis set used in this work. The basis set was taken from Neto *et al* [28]. Its original structure is 5s3p2d. For scattering, one p and one d functions were added.

Type	Exponent	Contraction coefficient
s	6711.76	0.001984
	1029.56	0.014862
	234.625	0.076129
	65.0861	0.286645
	20.6813	0.710844
s	7.35948	0.761736
	2.86133	0.268284
s	0.75772	1.000000
s	0.22278	1.000000
s	0.05511	1.000000
p	26.9531	0.018562
	6.01778	0.116576
	1.76063	0.381643
	0.56065	0.641238
p	0.17526	1.000000
p	0.04764	1.000000
p	0.02970	1.000000
d	0.89591	1.000000
d	0.24164	1.000000
d	0.09044	1.000000

virtual target excitations. The ground zero criterion for selection of a basis set is the description of selected molecular properties. Of special relevance to the calculations are the ground state energy, the quadrupole moment and the polarisation.

Among many tested basis sets, we elected the one shown in table 1 because it presented a reasonable description of the molecular parameters and was also able to satisfy the conditions for a good scattering calculation, to be described in subsection basis set validation.

The ground state wave function of the target was calculated in the equilibrium geometry configuration ($R_{NN} = 2.068\ a_0$), using the RHF approximation. The energy obtained in a SCF calculation was $-108.969\,954$ Hartrees. For scattering calculations, the description of the molecular charge distribution and how it responds to an external electric field are major points to be considered. These characteristics are incorporated by the quadrupole moment (Q) and the polarizability tensor components (α_0 and α_2), the last one receiving special attention in what concerns the internuclear separation dependence in the work of Temkin [29]. Tables 2 and 3 show the values obtained for these quantities with the basis set given in table 1. The values obtained for the quadrupole moment are comparable to the theoretical values reported by the two-dimensional numerical Hartree–Fock calculation of Sundholm *et al* [30] and the coupled-cluster singles and doubles (CCSD) result of Halkier *et al* [31]. The value obtained with basis 1 is ≈93% of the experimental value furnished by Graham *et al* [32], a variation we find acceptable

Table 2. Quadrupole moments of the CGF basis set given in table 1 compared to other experimental and theoretical values. The experimental value is the one reported by Graham *et al* [32]. The theoretical values are the ones given by the two-dimensional numerical Hartree–Fock calculation of Sundholm *et al* [30] and the CCSD calculation of Halkier *et al* [31].

References	Quadrupole moment (ea_0^2)
Basis 1	−0.967
Expt [32]	-1.03 ± 0.02
Theory-numerical HF [30]	−0.940
Theory-CCSD [31]	-1.12 ± 0.02

Table 3. Polarizability of the CGF basis set compared to other experimental and theoretical values. The theoretical are from a CI calculation of Langhoff *et al* [33] while the experimental are those reported by Bridge and Buckingham [34].

References	$\alpha_0\ (a_0^3)$	$\alpha_2\ (a_0^3)$
Basis 1	11.48	3.47
Expt [34]	11.92	3.13
Theory—CI [33]	11.52	3.16

taken the limitations of using a RHF molecular wave function. On the other hand, the components of the polarizability tensor show good agreement with the CI calculation of Langhoff *et al* [33]. A small difference is seen when we compare the values obtained to the experimental results of Bridge and Buckingham [34]. In spite of that, however, we consider this discrepancy tolerable for scattering calculations.

These two properties are of special attention because they are directly connected to the asymptotic form of the positron-N_2 scattering potential:

$$V \overset{x\to\infty}{\longrightarrow} \frac{Q}{x^3}P_2(\cos\theta) - \frac{1}{2}\left(\frac{\alpha_0}{x^4} + \frac{\alpha_2}{x^4}P_2(\cos\theta)\right), \qquad (6)$$

where x is the positron position and the θ is angle between the positron coordinate and the internuclear axis (see Morrison and Hay [35] and Morrison *et al* [36]). Note that only the parallel polarisability $\alpha_{zz} = \alpha_0 + \alpha_2 P_2 \cos\theta$ (the relations of the polarisability tensor can be found in reference [37]) contributes to the polarisation potential, the derivation of such component is given in appendix A. A description of the potential at the molecular border is an important ingredient in a rotational excitation calculation because, intuitively, it is expected that incident positrons with higher angular momenta, and consequently higher impact parameters, will transmit angular momentum to the molecule more effectively.

3. Results and discussions

We start with the validation of the CGF set used to compute the rotational excitation cross sections. After that, we present our results for the rotational cross sections and compare them to the ones previously reported by other authors.

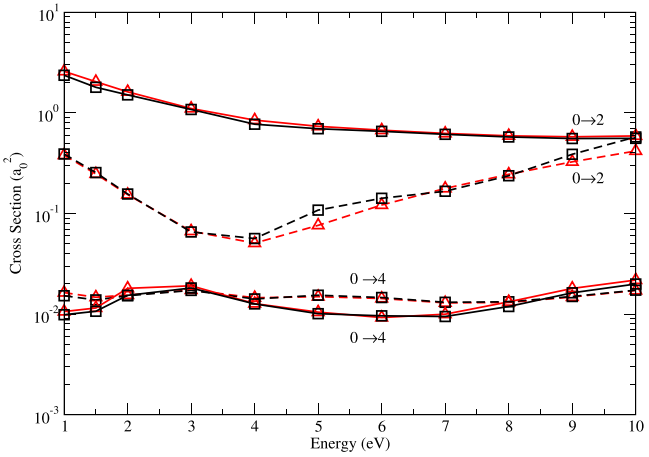

Figure 1. Convergence of k-insertion (σ^k) and $3dk$-insertion ($\sigma^{3\,dk}$) rotational excitation cross sections for transitions $0 \rightarrow 2$ and $0 \rightarrow 4$ in the static (ST) and static plus polarisation (SP) approximations. Legends are: dashed lines, static; full line: static plus polarisation; squares: σ^k; triangles: $\sigma^{3\,dk}$.

3.1. Basis set validation

An important point to consider when we analyse results from *ab initio* methods like SMC, is that, even though a CGF set is able to describe the molecular properties, it does not imply that it will also be an adequate basis set for scattering. It happens because the same molecular orbitals used to represent the molecule are also used to represent the positron scattering orbitals (see equation (5)). From the point of view of calculation of matrix elements and computational implementation it is a convenient choice. However, it may lead to several pathological linear dependencies. Due to this peculiar characteristic, we have adopted the same criteria used in Zanin *et al* [26]. For the sake of completeness, we repeat then in brief form here:

(I) $Z_{eff}^{BSBA} \approx Z$. Briefly, when the annihilation parameter Z_{eff} is computed considering a scattering basis set expansion that mimics the first Born approximation (known as the Basis Set Born Approximation), it must give values close to the number Z of electrons of the molecule [38, 39].

(II) $\sigma^k \approx \sigma^{3\,dk}$. The cross sections must be converged in relation to the method used to compute the Green's function matrix elements: σ^k and $\sigma^{3\,dk}$ denote cross sections computed with the k-insertion and $3dk$-insertion methods respectively [40].

In figure 1, we show the integral cross section (ICS) for transitions $J_i = 0 \rightarrow J_f = 2$ (quadrupole) and $J_i = 0 \rightarrow J_f = 4$ (hexadecapole), from now on simply denoted by $0 \rightarrow 2$ and $0 \rightarrow 4$, in the static (ST) and static plus polarisation (SP) approximations. The ICS associated to the quadrupole transition calculated in the SP approximation presents a higher magnitude than the corresponding one computed in the ST approximation for all energies. Such behaviour comes from the negative value of the quadrupole moment of the N_2 molecule (see table 2). In this situation, the Q and α_2 terms present at the molecular edge interfere constructively.

The ICS for the hexadecapole transition, on the other hand, has a very interesting peculiarity: it is practically the same computed considering or not the correlation-polarisation effects. As the own name suggests, this cross section is associated to the hexadecapole moment that comes primarily from the static potential. As we discuss at the end of the next subsection, the small discrepancies observed between the ST and SP calculations can be explained by the non-significant presence of terms of the form $P_4(\cos\theta)$ in the correlation-polarisation potential and, in the same way, by the different scattering wave functions generated in each of these approximations.

The convergence $\sigma^k \approx \sigma^{3\,dk}$ is evident and was used as a final criterion to choose the basis given in table 1.

3.2. Rotational cross sections

The measurement of rotational cross sections is still an open theme in the positron field, which it means that there are no experimental data for direct comparison with theory. In this circumstance, we compare our results with the theoretical works of Mukherjee *et al* [22], del Valle and Gianturco [5] and the more recent results of Mukherjee and Mukherjee [23]. The reason to do so is that it permits to analyse how the SMC-ARA cross sections compare to the close-coupling-model-potential results and, at the same time, to visualise the whole picture of the positron-N_2 rotational cross sections for energies just below the positronium formation threshold.

To model rotational cross sections, it is important to keep in mind that two ingredients are always present and have direct influence in the final results obtained. These are:

(i) the representation of the positron–molecule interaction;
(ii) the coupling between the vibrational and rotational states of the target.

In the close-coupling calculations with which we compare, the positron–molecule interaction is written as a single-body effective potential, given by the superposition of a static $V_{st}(\vec{x})$ and a correlation-polarisation component $V_{cp}(\vec{x})$ known as PCOP [41, 42]. In this approach, $V_{cp}(\vec{x})$ is given by

$$V_{cp}(\vec{x}) = \begin{cases} V_{corr}(\vec{x}) & x \leqslant r_c \\ V_{pol}(\vec{x}) = -\frac{\alpha_0}{2x^4} - \frac{\alpha_2}{2x^4} P_2(\cos\theta) & x \geqslant r_c. \end{cases} \quad (7)$$

In practice, $V_{corr}(\vec{x})$ describes the positron–molecule interaction when the positron is inside the molecular cloud. It is derived from the correlation energy of a positron in a homogeneous electron gas as described in density functional theory [43]. Explicit expressions for $V_{corr}(\vec{x})$ can be found in the articles of Mukherjee *et al* [22] and Gianturco *et al* [44]. $V_{pol}(\vec{x})$, as described earlier, is the polarisation component associated to the asymptotic form of the positron–molecule scattering potential (see equation (6)); r_c is a cut-off radius, defined by the value of the radial coordinate where $V_{corr}(\vec{x})$ and $V_{pol}(\vec{x})$ cross for the first time and it connects both components of $V_{cp}(\vec{x})$.

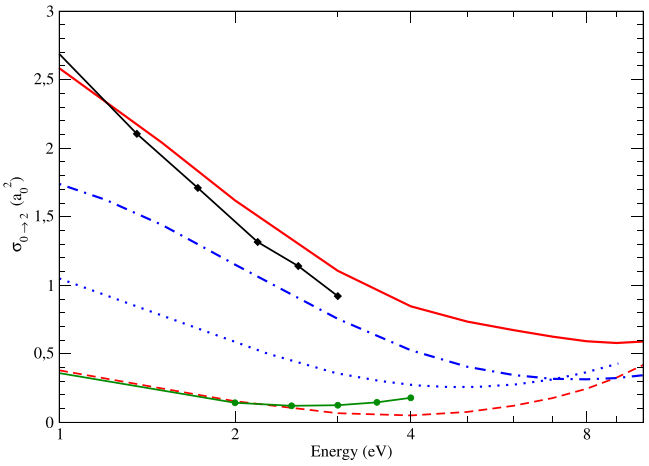

Figure 2. Comparison with other calculations for rotational transition $0 \rightarrow 2$. The legends are: solid line and dashed line, SP and ST of SMC; dashed–dotted line our PCOP calculation; solid line with circles, del Valle [5]; dotted line, Mukherjee *et al* [22] and solid line with diamonds, Mukherjee and Mukherjee [23]. Our results are summarized in table C1 of Appendix C.

In SMC, on the other side, except in the static approximation, the potential cannot be expressed as a simple single-body expression. In fact, it is the coupling between the potential and the trial vectors of the closed Q space, used to expand the scattering wave function, that in practice gives rise to the correlation-polarisation effects.

The coupling between the rotational states is taken since the start in the close-coupling formulations, making this aspect of the problem more precise in such models. The single-body effective potential that scatters the positron is expanded in a basis that, in principle, couple the vibrational (v) and rotational states of the molecule (j) with the angular momentum states of the positron (l): $\langle v'j'l'|V(\vec{x},\vec{R})|v''j''l''\rangle$. The dynamical coupling effect appears in solving the coupled differential equations where the solution of a particular channel depends on the influence of other channels.

In the methodology we considered here (SMC+ARA), the scattering amplitude (equation (3)) is calculated in the fixed-nuclei approximation, without considering any kind of coupling between the vibrational and rotational states of the target. Then, using the ARA, an effective expression to compute the rotational cross sections is derived, considering that the electronic and rotational states of the target are fully decoupled, a picture physically justifiable for 'high energy' positrons.

In figure 2 we show the $0 \rightarrow 2$ excitation cross section. The dashed and the solid lines are the ST and the SP polarisation results obtained in this work respectively. The dotted line is the result of Mukherjee *et al* [22] generated with a lab-frame close-coupling (LFCC) calculation. The solid line with circles is the result reported by del Valle and Gianturco with the space frame-rotational close-coupling (SF-RCC) [5] while the full line with diamonds is the cross section of Mukherjee and Mukherjee [23] considering a rovibrational close-coupling (RVCC) formulation. The dotted–dashed line is a calculation performed with the method of continued fractions (MCF) [27, 45] combining the PCOP with ARA. The LFCC and SF-RCC results were calculated in the rigid-rotor approximation, which means that the vibrational states $v(R)$ are simply not considered in the expansion of the scattering potential.

From figure 2, we immediately recognise that three previous different calculations performed with PCOP provide three different quadrupole rotational cross sections. The discrepancies between the rigid rotor calculations (LFCC and SF-RCC) can be explained by the different parameters used in the expansion of the potential and also by the different radial grids considered for integration. For example, in the LFCC calculation, the authors considered rotational states from $j = 0$ to $j = 10$ in the expansion of the scattering potential, but the equations were solved up to a total angular momentum $J_{\max} = 12$ ($\vec{J} = \vec{l} + \vec{j}$). The SF-RCC results, on the other hand, were performed with a more complete expansion, the multipolar coefficients of the potential expansion going to $\lambda_{\max} = 26$ and a maximum partial wave angular momenta for the scattering positron of $l_{\max} = 33$.

As stated previously, of paramount relevance for the description of the $0 \rightarrow 0$ and $0 \rightarrow 2$ cross sections are, respectively, the values of α_0 and α_2 considered. Mukherjee *et al* [22] used $\alpha_0 = 11.74$ a_0^3 and $\alpha_2 = 3.17$ a_0^3, values slightly different from the ones considered here (see table 3). Different choices of α_0 and α_2 affect the determination of the cut-off radius r_c (there is a cut-off radius for the spherical and another one for the anisotropic component of the potential), affecting the level of contribution of the correlation and generating different potentials for each set of parameters. The agreement between the SF-RCC and the static SMC+ARA $0 \rightarrow 2$ cross sections, mainly towards lower energies, suggests that the description of the polarisation used by these authors was unsatisfactory, or that, by some reason, the value used for the cut-off radius killed the contribution of the correlation-polarisation component, generating a potential practically equal to the static one.

Recently Mukherjee and Mukherjee [23] improved the LFCC model incorporating the vibrational states of the target in the expansion of the scattering potential. Our results apparently resemble the RVCC model of Mukherjee and Mukherjee [23] until 3 eV (higher energies are not reported). Such agreement seems strange due to the very different nature of the models. In our calculation, the correlation-polarisation effects comes from an *ab initio* description and the rotational dynamics is regarded from the combination of rigid rotor and adiabatic approximations. In the work of Mukherjee and Mukherjee [23], the correlation-polarisation effects are taken from a model potential approach and the vibrational and rotational dynamics are taken in full. Since several factors influence the behaviour and magnitude of the rotational cross sections, we performed the PCOP+ARA calculation, represented by the dashed–dotted line in figure 2, considering the basis set given in table 1. Under such conditions, the same molecular parameters (quadrupole and polarizability) and static components of the scattering potential are considered in both calculations. We see from figure 2, that the SMC cross section is systematically higher in magnitude and both have the same energy

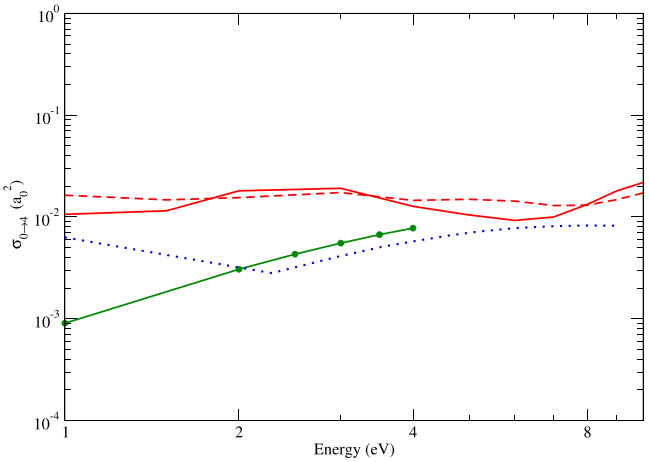

Figure 3. Comparison with other calculations for rotational transition $0 \rightarrow 4$. Our results are given in form of table in Appendix C, table C2. Legends are the same as figure 2.

dependency. It means that the difference between these rotational cross sections comes from the description of the correlation component of the interaction potential. This suggests that the incorporation of vibrational dynamics in the SMC calculation would also raise the magnitude of the rotational cross section. The magnitude of the effect is, of course, a theme for further investigation. At this moment, we can say that the apparent agreement with the RVCC results of Mukherjee and Mukherjee [23] is, in practice, fortuitous.

Finally, in figure 3 we present $0 \rightarrow 4$ cross sections obtained in this work and compare to LFCC [22] and SF-RCC [5] scattering models. Results for this transition were not reported in the RVCC model. Hexadecapole transitions depends, mainly, on terms of the form $P_4(\cos\theta)$ in the potential. The convergence between the ST and SP calculations just reinforce the fact that the magnitude of these terms is practically negligible in the correlation-polarisation potential. Some small discrepancies are expected, because the scattering wave function varies with the approximation used to compute the rotational cross section. In fact, we can easily visualise that there is no agreement between any of the different scattering models. In spite of the smaller magnitude associated to the hexadecapole cross section, this result simply shows that the situation about positron-N_2 rotational cross sections is far from being clarified.

Results for this transition were not reported in the RVCC model, such that we can only compare the SMC+ARA ones to the LFCC and the SF-RCC results. In fact, we can easily visualise that there is no agreement between any of the different scattering models. In spite of the smaller magnitude associated to the hexadecapole cross section, this result simply shows that the determination of the positron-N_2 rotational cross sections is far from being achieved.

4. Conclusion

The results reported in this article are, as far as we know, the first positron-N_2 rotational cross sections performed with an *ab initio* interaction approach. Rotational dynamics is treated within the rigid rotor and adiabatic approximations considering an *ab initio* correlation-polarisation potential.

The quadrupole transition exhibits fortuitous agreement with the rovibrational cross section of RVCC and shows to be higher when compared to other rigid rotor approximations. After performing our own model potential calculation, setting the same molecular parameters as SMC, we found that the discrepancies with the rigid rotor models and the agreement with the RVCC is explained through the difference in the correlation effects of each method. For the hexadecapole transition, the static and SP polarisation suggests that terms $\propto P_4(\cos\theta)$ are negligible in the computation of such transition.

Acknowledgments

M V Barp, E P Seidel and F Arretche would like to thanks the Programa de Pós-Graduação em Física of Universidade Federal de Santa Catarina for the support. M V Barp and E P Seidel would like to thanks the Conselho Nacional de Desenvolvimento Científico e Tecnológico for the financial support.

Appendix A. Asymptotic positron–molecule scattering potential and parallel polarisability

In this appendix, we show that the asymptotic form of the positron–molecule scattering potential is due to the parallel component of the polarisability tensor (see equation (6)).

From the many-body formulation, the electrostatic interaction between a positron and a diatomic homonuclear molecule (like N_2, H_2, …) can be expressed in atomic units, by

$$V(\vec{x}, \vec{r}_j, \vec{R}_A) = \sum_A \frac{\mathcal{Z}_A}{|\vec{x} - \vec{R}_A|} - \sum_j \frac{1}{|\vec{x} - \vec{r}_j|}, \qquad \text{(A.1)}$$

where $\vec{x}$ is the positron coordinate, $\vec{r}_j$ is the set of electronic coordinates, $\vec{R}_A$ is the set of nuclear coordinates and $\mathcal{Z}_A$ stands for the atomic number.

Using the optical potential technique[3], the Schrodinger equation for a diatomic homonuclear molecule placed in the field of a fixed positron at $\vec{x}$ is

$$[\mathcal{H}_{mol} + V(\vec{x}, \vec{r}_j, \vec{R}_A)]\Phi(\vec{x}, \vec{r}_j, \vec{R}_A) = E(\vec{x})\Phi(\vec{x}, \vec{r}_j, \vec{R}_A), \qquad \text{(A.2)}$$

where $\mathcal{H}_{mol}$ is the molecular Hamiltonian.

Asymptotically, as $x \rightarrow \infty$, one can consider that the solution of equation (A.2) is the unperturbed molecular ground state wave function, i.e., $\Phi(\vec{x}, \vec{r}_j, \vec{R}_A) \rightarrow \Phi_0(\vec{r}_j, \vec{R}_A)$ and $E(\vec{x}) \rightarrow E^{(0)}$, where $E^{(0)}$ is the ground state energy of the molecule. In order to find the corrections on the energy, we

[3] See section 12.2, equation (12).41, of [46].

can apply perturbation theory. Therefore, up to second order,

$$E(\vec{x}) = E^{(0)} + E^{(1)}(\vec{x}) + E^{(2)}(\vec{x}). \tag{A.3}$$

Note that, from equation (A.1), the first-order correction

$$E^{(1)}(\vec{x}) = \langle \Phi_0(\vec{r}_j, \vec{R}_A)|\, V(\vec{x}, \vec{r}_j, \vec{R}_A)|\Phi_0(\vec{r}_j, \vec{R}_A)\rangle \tag{A.4}$$

is the static interaction of a positron with the molecule.

The second-order correction is given by

$$E^{(2)}(\vec{x}) = \sum_{N\neq 0} \frac{|\langle \Phi_0(\vec{r}_j, \vec{R}_A)|\, V(\vec{x}, \vec{r}_j, \vec{R}_A)\, |\Phi_N(\vec{r}_j, \vec{R}_A)\rangle|^2}{E_0 - E_N}. \tag{A.5}$$

We now pay attention to the term $\langle \Phi_0|V|\Phi_N\rangle$ of equation (A.5). Applying the multipole expansion in equation (A.1), the potential is rewritten as

$$V(\vec{x}, \vec{r}_j, \vec{R}_A) \xrightarrow{x\to\infty} \sum_A \sum_\lambda \mathcal{Z}_A \frac{R_A^\lambda}{x^{\lambda+1}} P_\lambda(\hat{R}_A.\hat{x}) - \sum_j \sum_\eta \frac{r_j^\eta}{x^{\eta+1}} P_\eta(\hat{r}_j.\hat{x}), \tag{A.6}$$

where P_λ and P_η are the Legendre polynomials with the respective multipole expansion index. Then, from equations (A.6) and $\langle \Phi_0|V|\Phi_N\rangle$ of equation (A.5),

$$\langle \Phi_0|V|\Phi_N\rangle = \langle \Phi_0(\vec{r}_j, \vec{R}_A)| \times \sum_A \left(\frac{\mathcal{Z}_A}{x} + \mathcal{Z}_A \frac{R_A}{x^2} P_1(\hat{R}_A.\hat{x}) + \ldots\right) - \sum_j \left(\frac{1}{x} + \frac{r_j}{x^2} P_1(\hat{r}_j.\hat{x}) + \ldots\right)|\Phi_N(\vec{r}_j, \vec{R}_A)\rangle. \tag{A.7}$$

Considering the orthonormality of the molecular states and taking into account only the first non-vanishing term of the multipole expansion we have,

$$\langle \Phi_0|V|\Phi_N\rangle = \langle \Phi_0(\vec{r}_j, \vec{R}_A)|\sum_A \left(\mathcal{Z}_A \frac{R_A}{x^2} P_1(\hat{R}_A.\hat{x})\right) - \sum_j \left(\frac{r_j}{x^2} P_1(\hat{r}_j.\hat{x})\right)|\Phi_N(\vec{r}_j, \vec{R}_A)\rangle. \tag{A.8}$$

Without loss of generality, we may consider the positron along the $\hat{z}$ axis, consequently

$$\langle \Phi_0|V|\Phi_N\rangle = \frac{1}{x^2}\langle \Phi_0(\vec{r}_j, \vec{R}_A)|\sum_A \mathcal{Z}_A z_A - \sum_j z_j|\Phi_N(\vec{r}_j, \vec{R}_A)\rangle. \tag{A.9}$$

Note that $\sum_A \mathcal{Z}_A z_A - \sum_j z_j = \mu_z$ is the dipole operator in the many-body formulation[4]. Since the dipole polarisability is given by

$$\alpha_{ij} = 2\sum_{N\neq 0} \frac{\langle \Phi_0|\mu_i|\Phi_N\rangle\langle \Phi_N|\mu_j|\Phi_0\rangle}{E_0 - E_N}, \tag{A.10}$$

thereupon, from the second-order correction on the energy (A.5) and the dipole polarisability (A.10), we identify that, asymptotically,

$$V_{pol} \sim -\frac{\alpha_{zz}}{2x^4} = -\frac{\alpha_0}{2x^4} - \frac{\alpha_2}{2x^4} P_2(\cos\theta), \tag{A.11}$$

the negative sign (attractive character of the polarisation potential) comes from the fact that $E_0 - E_N < 0$. Hence, only the parallel polarisability contributes to the asymptotic potential.

[4] See section 2.3 of [47].

Appendix B. Non-adiabatic and adiabatic polarisabilities

In this appendix, we briefly discuss why we use adiabatic polarisabilities, instead of non-adiabatic ones, in our calculations.

The polarisability has been studied [48] adiabatically (considering the Born–Oppenheimer approximation) and non-adiabatically (taking into account the nuclear degrees of freedom). Recently, the adiabatic and non-adiabatic (hyper) polarisabilities have been investigated [49] for diatomic systems.

The effects associated to the non-adiabatic polarisabilities can be relevant mainly when the dependence with the inter-nuclear separation is considered. This is mandatory to the computation of vibrational cross sections and it may influence the results, as demonstrated in [29] for electron-N_2 scattering. In fact, the difference of the adiabatic and non-adiabatic treatments for vibrational cross sections of positron-N_2 have been evaluated [50]. As commented in the work of Tiihonen *et al* [49], a complete non-adiabatic calculation is limited to three particles only, thorough the Hylleraas basis approach [51].

The rotational cross sections reported in this article were performed in the Rigid Rotor combined to the ARA. In ARA, the rotational and electronic degrees of freedom are totally decoupled by virtue of the physical assumptions involved and the input data is the fixed-nuclei scattering amplitude. In SMC, the polarisabilities come from the Gaussian basis set used to represent the target wave function, while in MCF-PCOP the polarisabilities are input parameters. The polarisabilities provided by the basis set used in SMC were used in the MCF-PCOP calculations in order to clarify the influence over the rotational cross sections for different values of the polarisation in both models.

The majority of the models for electron-molecule or positron–molecule scattering work in the Born–Oppenheimer approximation. In this framework, the electronic and nuclear degrees of freedom are decoupled. Therefore, it is natural to use the adiabatic polarisabilities in the present calculations, first for a question of consistence and coherence, and second, because the comparison to the experimental values is reasonable (see table 3).

Table C1. Results of 0 → 2 rotational cross section for positron-N_2 in units of a_0^2.

Energy (eV)	SMC (ST)	SMC (SP)	MCF+PCOP
1.0	0.3798	2.5845	1.7394
1.2			1.6243
1.5	0.2472	2.0402	1.4403
1.7			1.3159
2.0	0.1541	1.6194	1.1512
3.0	0.0668	1.1058	0.7550
4.0	0.0508	0.8468	0.5265
5.0	0.0763	0.7348	0.4053
6.0	0.1215	0.6729	0.3452
7.0	0.1775	0.6251	0.3174
8.0	0.2453	0.5919	0.3140
9.0	0.3262	0.5788	0.3232
10.0	0.4181	0.5899	0.3441

Table C2. Results of 0 → 4 rotational cross section for positron-N_2 in units of $10^{-2}\ a_0^2$.

Energy (eV)	SMC (ST)	SMC (SP)
1.0	1.6348	1.0606
1.5	1.4717	1.1508
2.0	1.5474	1.8053
3.0	1.7360	1.9141
4.0	1.4548	1.2727
5.0	1.4928	1.0468
6.0	1.4310	0.9253
7.0	1.2946	0.9982
8.0	1.3059	1.3252
9.0	1.4796	1.8016
10.0	1.7198	2.1825

Appendix C. Rotational cross sections results

This appendix presents the rotational cross sections calculated with the methods SMC and MCF+PCOP in the form of tables.

ORCID iDs

Marcos V Barp https://orcid.org/0000-0002-6842-5633

References

[1] Deutsch M 1953 Annihilation of positrons *Prog. Nucl. Phys.* **3** 131
[2] Green J and Lee J 1964 *Positronium Chemistry* (New York: Academic) (https://doi.org/10.1016/B978-1-4832-3246-1.50010-9)
[3] Charlton M and Humberston J W 2001 *Positron Physics* (Cambridge: Cambridge University Press) (https://doi.org/10.1017/CBO9780511535208)
[4] Sharma S K, Sudarshan K and Pujari P K 2014 Unravelling the surface chemical characteristics and nanostructure of MgO/NiO catalyst using positronium probe: positron annihilation lifetime and age momentum correlation study *RSC Adv.* **4** 14733–9
[5] del Valle J A S and Gianturco F A 2005 Collisional heating of molecular rotations by positron impact: a computational analysis of the quantum dynamics *Phys. Chem. Chem. Phys.* **7** 318
[6] Sharma S K, Prakash J, Bahadur J, Sudarshan K, Maheshwari S, Mazumder S and Pujari P K 2014 Investigation of nanolevel molecular packing and its role in thermo-mechanical properties of PVA-FMWCNT composites: positron annihilation and small angle x-ray scattering studies *Phys. Chem. Chem. Phys.* **16** 1399–408
[7] Al-Qaradawi I, Charlton M, Borozan I, Whitehead R and Borozan I 2000 Thermalization times of positrons in molecular gases *J. Phys. B: At. Mol. Opt. Phys.* **33** 2725
[8] Blanco F *et al* 2016 Scattering data for modelling positron tracks in gaseous and liquid water *J. Phys. B: At. Mol. Opt. Phys.* **49** 145001
[9] Charlton M, Giles T, Lewis H and van der Werf D P 2013 Positron annihilation in small molecules *J. Phys. B: At. Mol. Opt. Phys.* **46** 195001
[10] Tao S J 1970 Annihilation of positrons in nitrogen *Phys. Rev.* A **2** 1669
[11] Coleman P G, Griffith T C and Heyland G R 1974 Measurement of total scattering cross-sections for positrons of energies 2400 ev on molecular gases: H_2, D_2, N_2, CO *Appl. Phys.* **4** 89
[12] Griffith T C and Heyland G R 1978 Experimental aspects of the study of the interaction of low-energy positrons with gases *Phys. Rev.* **39** 169
[13] Sharma S C and McNutt J D 1978 Positron annihilation in gaseous nitrogen and nitrogen-neon mixtures at 77 K *Phys. Rev.* A **18** 1426
[14] Murphy T J and Surko C M 1992 Positron trapping in an electrostatic well by inelastic collisions with nitrogen molecules *Phys. Rev.* A **46** 5696
[15] Coleman P G, Griffith T C and Heyland G R 1981 Rotational excitation and momentum transfer in slow positron-molecule collisions *J. Phys. B: At. Mol. Phys.* **14** 2509
[16] Natisin M R, Danielson J R and Surko C M 2015 Formation of buffer-gas-trap based positron beams *Phys. Plasma* **22** 033501
[17] Marjanovic S and Petrovic Z L 2017 Monte Carlo modeling and optimization of buffer gas positron traps *Plasma Sources Sci. Technol.* **26** 024003
[18] Natisin M R, Danielson J R and Surko C M 2014 Positron cooling by vibrational and rotational excitation of molecular gases *J. Phys. B: At. Mol. Opt. Phys.* **47** 225209
[19] Hara S 1972 Behaviour of positrons in molecular gases: I. Rotational excitation of molecules by slow positrons *J. Phys. B: At. Mol. Phys.* **5** 589
[20] Darewych J W and Baille P 2014 Comparison of one and two centre studies of low energy scattering by diatomic molecules *J. Phys. B: At. Mol. Opt. Phys.* **7** 1
[21] Gillespie E S and Thompson D G 1975 Positron scattering by molecular nitrogen *J. Phys. B: At. Mol. Phys.* **8** 2858
[22] Mukherjee T, Ghosh A S and Jain A 1991 Low-energy positron collisions with H_2 and N_2 molecules by using a parameter-free positron-correlation-polarization potential *Phys. Rev.* A **43** 2538
[23] Mukherjee T and Mukherjee M 2015 Low-energy positronnitrogen-molecule scattering: a rovibrational close-coupling study *Phys. Rev.* A **91** 062706
[24] Germano J S E and Lima M A P 1993 Schwinger multichannel method for positron-molecule scattering *Phys. Rev.* A **47** 3976
[25] Chang E S and Temkin A 1969 Rotational excitation of diatomic molecules by electron impact *Phys. Rev. Lett.* **23** 399

[26] Zanin G, Tenfen W and Arretche F 2016 Rotational excitation of H_2 by positron impact in adiabatic rotational approximation *Eur. Phys. J.* D **70** 179
[27] Tenfen W, Mazon K, Michelin S and Arretche F 2012 Low-energy elastic positron cross sections for H_2 and N_2 using an *ab initio* target polarization *Phys. Rev.* A **86** 042706
[28] Neto A C, Muniz E P, Centoducatte R and Jorge F E 2005 Gaussian basis sets for correlated wave functions. Hydrogen, helium, first- and second-row atoms *Phys. Rev.* A **718** 219
[29] Temkin A 1978 Internuclear dependence of the polarizability of n_2 *Phys. Rev.* A **17** 1232–5
[30] Sundholm D, Pyykko P and Laaksonen L 1985 Two-dimensional, fully numerical molecular calculations: X. Hartree-Fock results for He_2, Li_2, Be_2, HF, OH^-, N_2, CO, BF, NO^+ and CN^- *Mol. Phys.* **56** 1411
[31] Halkier A, Coriani S and Jorgensen P 1998 The molecular electric quadrupole moment of N2 *Chem. Phys. Lett.* **294** 292
[32] Graham C, Imrie D A and Raab R E 1998 Measurement of the electric quadrupole moments of CO_2, CO, N_2, CL_2 and BF_3 *Mol. Phys.* **93** 49
[33] Langhoff S R, Bauschlicher C W and Chong D P 1983 Theoretical study of the effects of vibrational rotational interactions on the raman spectrum of N_2 *J. Chem. Phys.* **78** 5287
[34] Bridge N J and Buckingham A D 1966 The polarization of laser light scattered by gases *Proc. R. Soc.* A **295** 334
[35] Morrison M A and Hay P J 1979 *Ab initio* adiabatic polarization potentials for low-energy electron-molecule and positronmolecule collisions: the e-N_2 and e-CO_2 systems *Phys. Rev.* A **20** 740
[36] Morrison M A, Feldt A N and Austin D 1984 Adiabatic approximations for the nuclear excitation of molecules by low-energy electron impact: rotational excitation of H_2 *Phys. Rev.* A **29** 5
[37] Belfiore L A 2010 *Physical Properties of Macromolecules* (New York: Wiley) (https://doi.org/10.1002/9780470551592)
[38] do M T, Varella N, de Carvalho C R C and Lima M A P 2002 The Schwinger multichannel method (SMC) calculations for z_{eff} were off by a factor of *z Nucl. Instrum. Methods Phys. Res.* B **192** 225
[39] Arretche F and Lima M A P 2006 Electronic excitation of H_2 by positron impact *Phys. Rev.* A **74** 042713
[40] Lima M A P, Brescansin L M, da Silva A J R, Winstead C and McKoy V 1990 Applications of the Schwinger multichannel method to electron-molecule collisions *Phys. Rev.* A **41** 327
[41] Jain A 1990 Low-energy positron-argon collisions by using parameter-free positron correlation polarization potentials *Phys. Rev.* A **41** 2437
[42] Jain A 1990 A treatment of low-energy positron-co collisions using a new parameter-free positron correlation polarisation (PCOP) potential *J. Phys. B: At. Mol. Opt. Phys.* **23** 863
[43] Boronsky E and Nieminen R M 1986 Electron-positron density-functional theory *Phys. Rev.* B **34** 3820
[44] Gianturco F A, Mukherjee T and Paioletti P 1997 Positron scattering from polar molecules: rotovibrationally inelastic collisions with CO targets *Phys. Rev.* A **56** 3638
[45] Horáček J and Sasakawa T 1983 Method of continued fractions with application to atomic physics *Phys. Rev.* A **28** 2151
[46] Bransden B H and Joachain C J 1983 *Physics of Atoms and Molecules* 1st edn (Essex: Longman)
[47] Stone A J 2013 *The Theory of Intermolecular Forces* 2nd edn (Oxford: Oxford University Press) (https://doi.org/10.1093/acprof:oso/9780199672394.001.0001)
[48] Bishop D M 1990 Molecular vibrational and rotational motion in static and dynamic electric fields *Rev. Mod. Phys.* **62** 343–74
[49] Tiihonen J, Kylänpää I and Rantala T T 2015 Adiabatic and nonadiabatic static polarizabilities of H and H_2 *Phys. Rev.* A **91** 062503
[50] Danby G and Tennyson J 1991 R-matrix calculations of vibrationally resolved positron-N_2 scattering cross sections *J. Phys. B: At. Mol. Opt. Phys.* **24** 3517
[51] Tang L-Y, Yan Z-C, Shi T-Y and Babb J F 2014 High-precision nonadiabatic calculations of dynamic polarizabilities and hyperpolarizabilities for low-lying vibrational-rotational states of hydrogen molecular ions *Phys. Rev.* A **90** 012524